Steady-State Movement Related Potentials for Brain Computer Interfacing

Kianoush Nazarpour*, *Member, IEEE,* Peter Praamstra, R. Chris Miall, and Saeid Sanei, *Senior Member, IEEE*

***Abstract*— An approach for brain computer interfacing (BCI) by analysis of steady-state movement related potentials (ssMRP) produced during rhythmic finger movements is proposed in this paper. The neurological background of ssMRPs is briefly reviewed. Averaged ssMRPs represented the development of a lateralized rhythmic potential and the energy of the electroencephalogram (EEG) signals at the finger tapping frequency can be used for single trial ssMRP classification. The proposed ssMRP-based BCI approach is tested using the classic Fisher's linear discriminant (FLD) classifier. Moreover, the influence of the current source density transform on the performance of BCI system is investigated. The averaged correct classification rates (CCR) as well as averaged information transfer rates (ITR) for different sliding time windows are reported. Reliable single trial classification rates of 88%-100% accuracy are achievable at relatively high ITRs. Furthermore, we have been able to achieve CCRs of up to 93% in classification of the sMRPs recorded during imagined rhythmic finger movements. The merit of this approach is in the application of rhythmic cues for BCI, the relatively simple recording setup, and straightforward computations which make the real-time implementations plausible.**

***Index Terms*—Brain computer interfacing, electroencephalogram, steady-state movement related potentials.**

I. Introduction

MOVEMENT related brain activity has been studied for many years by means of readiness potentials (RPs) [1]. The RP is typically recorded during execution of self-paced voluntary movements. The contralaterally dominant part of movement related brain activity preceding movement is called lateralized readiness potential (LRP) [2]. This may be computed by subtraction of slow EEG potentials recorded ipsilaterally to the side of movement from potentials recorded contralaterally, followed by averaging of resultant potentials associated with left and right finger movements [3]. Temporal and spatial characteristics of averaged RPs and LRPs have been well investigated in cognitive and clinical neuroscience studies [1], [4].

Asymmetric RPs during discrete finger movements are readily recordable from almost all subjects, i.e. see [1] where pioneering studies showed that RP can be detected several hundred milliseconds prior to an overt movement. It has been concluded [1], [5], [6] that the asymmetric spatial distribution of these scalp potentials reflects motor preparation for a specific effector. The simple nature of RP signals has made them fairly effective for BCI applications [7], [8]. For instance, the Berlin and Tübingen BCI research groups have achieved above 90% correct binary classification rates [7]–[11] by developing various methodological and mathematical techniques. Despite the outstanding BCI performances by means of RPs, the use of such an approach is limited when compared to the P300- and the μ rhythm-based BCI protocols. There are several issues limiting the applicability of RPs; first, the inevitable DC drifts in EEG measurements due to sweating or electrode displacements, especially if the experiments become lengthy. Second, several low frequency artifacts such as postural changes, respiration and DC drifts within short data windows of 0.5 second length before the movement onset reduce the signal (RP) to noise ratio. In addition, after segmenting the recorded EEGs, a baseline removal stage is needed [8]. Although finding a short reference interval can be straightforward in offline analysis, the identification of such a reference interval within the online EEG stream is troublesome in real-time applications. Another problem arises from the nature of the RP: in order to allow the RP build up over time, the inter-movement interval should be several seconds [1]. Recent BCI studies, such as in [8], [12], have attempted to modify the conventional RP-based BCI paradigms by instructing the subjects to tap at faster paces than usual. The information transfer rate (ITR) - measured in bits per minute (bpm) [13], [14] - was increased. However, faster tapping led to decrement of the correct classification rates (CCRs). For instance, as reported in [12], in binary classification of RP features, the mis-classification increased from 5% (ITR [bpm] $\approx$ 18.6) to 19% (ITR [bpm] $\approx$ 52.9) when the inter-tap intervals (ITI) dropped from 2 to 0.5 seconds.

An alternative approach for BCI based on ssMRPs is presented here which overcomes the above difficulties and provides desirable classification rates in a high ITR framework. It does not imply any extra computational load and therefore, its real-time implementation is possible.

This paper is organized as follows. In Section II, we first briefly review the conventional applications of brain steady-state visual evoked potentials (ssVEP) for BCI. The main motivation and the neurological background of using ssMRPs for BCI applications are then presented. In Section III, we propose an effective ssMRP recording protocol suitable for real-time BCI applications and explain the two experiments we carried out. Then, the pre-processing, feature extraction,

Manuscript received September 03, 2008; revised January 26, 2009; revised April 03, 2009. This work is supported by The Wellcome Trust, UK. The work of S. Sanei is supported by The Leverhulme Trust, UK. *Asterisk indicates the corresponding author.*

*K. Nazarpour was with the Centre of Digital Signal Processing, Cardiff University, UK. He is now with the Behavioural Brain Sciences Centre, School of Psychology, University of Birmingham, Birmingham, B15 2TT, UK. (e-mail: K.Nazarpour@bham.ac.uk).

P. Praamstra and R. C. Miall are with the Behavioural Brain Sciences Centre, School of Psychology, University of Birmingham, Birmingham, B15 2TT, UK.

S. Sanei is with the Centre of Digital Signal Processing, School of Engineering, Cardiff University, Cardiff CF24 3AA, UK.

and classifier design stages are described. Section IV reports the results where the spatio-temporal characteristics of the averaged ssMRPs will be first presented. We subsequently report the results of our BCI scheme during the movement initiation and the synchronization states and also during the course of the trials. We further investigate the effect of the time window size on the BCI performance in Section IV-C. In Section IV-D, we consider the effect of the co-existing transient visual evoked potentials (VEPs) on ssMRP measurements. The applicability of ssMRP-based BCI in real-life rehabilitation problems and its extension to motor imagery BCI are then discussed in this section. Moreover in section IV-F, we investigate how successful the subjects are in maintaining the correct rhythm when the taps are carried out without the visual cues. Section V presents the concluding remarks.

II. Brain Steady-State Potentials for BCI

Conventionally, in steady-state potential based BCI, users are exposed to rhythmic visual or audio cues. For instance, in the increasingly important steady-state visual evoked potentials (ssVEP)-based BCI system, bilaterally distributed visually evoked brain potentials are recorded from the visual cortex. Since the fundamental frequency of the stimulation [15], [16] and its first few harmonics [17] are dominant spectral components of the recorded EEG, multi-class BCIs may be realized without extensive subject training [18]. In an ssVEP-based BCI, in order to have an output the user has to shift their gaze to the flashing stimulation corresponding to the task of interest and hence the BCI would be limited to recovering eye position or the direction of attention[1]. The ssVEP-based BCIs may potentially be unpleasant for the users who have to attend the repetitive high-frequency (usually about 10 Hz) flashing visual stimuli for the BCI to generate continuous outputs.

The objective of this paper is therefore, to introduce a high performance BCI methodology based on steady-state finger *movement* related potentials, independent of eye direction. In this approach, low-frequency (2 Hz) flashing visual stimuli are exploited and the subjects are asked to tap in synchrony with them rather than to gaze at them. It has been shown [1] that readiness potentials of about 2 Hz are EEG correlates of voluntary movement preparation. Therefore, as a prime candidate we used this frequency. Repp [20] in his extensive behavioral experiments has shown that sensorimotor synchronization to visual cues of up to maximum 3 Hz is possible. However, when audio signals are used the synchronization may be maintained up to relatively higher frequencies of up to 7-8 Hz. However, in the BCI context it is fair to say that ssMRPs do not have the broad frequency range of ssVEPs and whether EEG potentials generated by tapping with higher frequencies would be classifiable on the single-trial basis is subject to further research.

Execution of simple unimanual repetitive finger movements is associated with activity within the Rolandic fissure of the contralateral hemisphere corresponding to the primary sensorimotor cortex [21]. Our extensive behavioral neuroimaging studies on rhythmic movements have led to the hypothesis that there are distinct brain structures which perform *automatic* vs. *cognitively controlled* timing for repetitive movements [22], [23]. The automatic control (AC) system is primarily involved in continuous movements with frequencies greater than 1 Hz, i.e. sub-second intervals. It is likely to employ neural assemblies within the primary motor system. Furthermore, we have concluded that once a fast rhythmic task is selected and initiated, it may be executed without direct attention [24]. The timing control of a continuous series of fast and predictable movements should therefore require attention merely during the selection and initiation phases. On the other hand, the cognitively controlled (CC) timing system is more exploited in controlling movements at intervals much longer than 1s, i.e. at < 1 Hz frequencies. The CC timing structure requires the activation of additional lateralized prefrontal and parietal lobe structures.

Schaal *et al*. in [25] have verified that in discrete single-joint movements higher brain functions such as working memory (the dorsolateral prefrontal cortex), recall (the ventrolateral prefrontal cortex), and attention (the intraparietal sulcus and inferior parietal lobe) may be involved. In contrast, rhythmic movements show much less cerebral activity; the only significantly active region is the contralateral motor cortex. Intuitively, one would assign the AC system for timing of rhythmic movements and the CC systems for discrete movements.

Conventionally in BCI, subjects are instructed to move (imagine the movement of) their finger on a discrete-time basis. In contrast, it is hypothesized here that during fast rhythmic finger tapping, the AC timing system is involved and hence ssMRPs are confined to the contralateral sensorimotor cortex. This, in turn, implies that non-rhythmic motor related activities emanating from frontal cortex will be attenuated. Therefore, if a motor task is carried out (real or imaginary) synchronized to a rhythmic (2 Hz) stimulus, the neural responses (ssMRPs) will oscillate at the same frequency and hence, there should be a peak in the power spectrum of the recorded EEGs at the frequency of the oscillatory cue (and possibly its harmonics). Interestingly, this peak can represent a carrier frequency by which the EEGs are modulated. If the oscillations shows stronger amplitudes on the hemisphere contralateral to the moving finger, the ssMRP can be regarded as a potential signal for BCI applications.

III. Method

Two experiments were conducted to test the ssMRP-based BCI in practice. First, we recorded ssMRPs during repetitive *real* finger movements. In the second experiment, we further investigated the potential and limitations of the ssMRPs-based BCI. Specifically, we address the three following issues. First, we document the transient effect of the visually evoked potentials (VEP) caused by repetitive visual stimuli on the proposed BCI system. Second, we discuss how the proposed method is extensible to imagined movements. The classification scores of EEGs recorded during imagined rhythmic movement are presented following a short overview of the rhythmic modulation of cortical potentials by imagined tapping. Third, repetition

[1]Recently, Kelly *et al.* in [19] have reported a ssVEP-based BCI independent from gaze direction by classification of VEPs recorded during visual spatial attention.

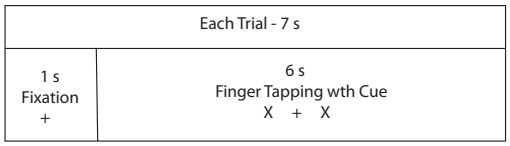

Fig. 1. Temporal structure of each trial; first dataset.

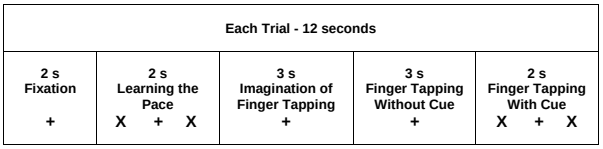

Fig. 2. Temporal structure of each trial; second dataset.

of a movement at an exact pace usually relies on an external stimulus - at least in the initiation and synchronization stages. This limitation can constrain the "real-life" applicability of the ssMRP-based BCI machines. We therefore recorded ssMRPs but without presenting the visual cues to objectively investigate to what extent a learnt pace can be maintained. EEG analysis, i.e. pre-processing and classification, in these two scenarios are the same as those addressed in experiment I.

A. Experiment 1: Real Movements

Five right-handed healthy individuals (one female) (age 33± 9) participated in the first experiment. They had normal or corrected-to-normal vision, with no apparent motor problems, and no previous BCI experience. All gave informed consent. Subjects I and III had previous musical training.

In this experiment EEG signals were recorded during rhythmic left or right finger tapping. The experiment was run in a quiet, normally illuminated room. The participants were seated comfortably in an armchair with the forearms placed on the armrests of the chair. Two force transducers were attached to the armrests, on top of which the participants held their index fingers of each hand. The stimuli were presented in white against a grey background on a 17 inch monitor at a resolution of 800×600. The viewing distance was set to 100 cm.

The Ag/AgCl scalp electrodes were placed according to the 10-5 system [26] using a carefully positioned nylon cap. The EEG potentials were recorded continuously with 128 electrodes relative to an (off-line) averaged left and right mastoid reference. The eye-movements and blinks were monitored by bipolar horizontal and vertical electro-oculogram (EOG) derivations. The EEG and EOG signals were amplified with a bandpass of 0-128 Hz using a BioSemi Active-Two amplifier and sampled at 512 Hz.

Each of five subjects first underwent a practice block of 20 trials. The main recording session comprised of eight blocks, each contained 40 trials, resulting in 320 trials for further analysis. The trial temporal structure is illustrated in Fig. 1. Each trial lasted 7 seconds which included one second for initial fixation and another 6 seconds for EEG recording during rhythmic tapping. In the first second of each trial a fixation cross "+" was shown in the center of the screen. Subsequently, while the cross was kept constant in the center, two rhythmically flashing "X"s appeared at the left and right sides of the cross for 6 seconds; each was 10 cm away from the center. The flashing frequency was set to 2 Hz. The participants were instructed to tap on one of the force sensors under left or right index fingers at a constant rate of 2 Hz in time with the flashing cues. The rest interval between trials was approximately one and half seconds, randomly changing with a variance of 150 milliseconds, so that the subjects would not guess the start of next trial. The choice between right or left finger tapping was made freely by the participants in each trial. However, they were asked to be fair between right and left responses. Therefore, on average we collected almost equal number of trials in each class across subjects.

The main reason for showing the flashing cues was to give the subjects a 2 Hz pace. Equidistant visual cues on either side from the center should not cause asymmetrically distributed potentials over the motor cortex. Moreover, the subjects were asked to maintain fixation on the central cross during the course of tapping. Later in Section IV-D, we show how eye-fixation and inattention to the cues should attenuate the stimulus-driven VEPs. Force transducers were utilized instead of conventional response switches in order to provide a setup in which the subjects did not actually press any switch, just performed repetitive tapping, which maintained the continuity of the repetitive finger movement.

B. Experiment 2: Imaginary Movements

In this experiment we investigated ssMRPs generated during imaginary movements. One right-handed healthy male (age 32) who did not have any BCI experience took part in this study; he had not participated in the first experiment. The EEG recording hardware setup was as described earlier in Section III-A. The recording session was comprised of eight blocks, each contained 30 trials, resulting in 240 trials for further analysis; almost equal number of trials for left and right fingers were recorded. This subject also first underwent a practice block of 20 trials.

The trial temporal structure is illustrated in Fig. 2. Each trial lasted 12 seconds which included 2 seconds for initial fixation and 2 second for synchronizing the correct 2 Hz pace with the visual cues. Next followed a 3 second period when imagined rhythmic finger movement were carried out. Next came another 3 second period when the subject was instructed to make real tapping movement, but without the rhythmic visual cues on the screen. In the final 2 seconds, the visual cues re-appeared on the screen to give a feedback on synchronization. The subject was asked to continue tapping in time with the cues; this data was not analyzed. Throughout the 12 seconds the fixation cross was maintained in the middle of the screen and the participant was asked to maintain fixation throughout the trial. Note that the switching time between the third stage (imagination of movement) and the fourth stage (real tapping without cue), was instructed to the subject by replacing the central fixation cross "+" with an "X" for 100 milliseconds.

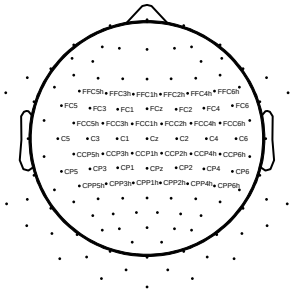

Fig. 3. The 45 electrodes over the sensorimotor cortex which were included in the classification.

C. Preprocessing

The EEG preprocessing was performed off-line using BrainVision Analyzer, Brain Products GmbH. Continuous EEG recordings were off-line segmented in epochs from 1-7 s after the trial onset in the first and 2-10 s in the second set of measurements. Specifically, we followed a dual-stage artifact rejection procedure: first, all trials in which the absolute difference between the maximum and minimum values of each vertical EOG channels was greater than 100 μV were rejected. Then, we visually searched and rejected the trials in which other artifacts, e.g. body/eye movements or electrode displacements, were evident.

On average respectively, 15% and 10% of trials were rejected in the first and second experiments. Multi-channel EEG measurements from scalp electrodes were then narrow bandpass filtered between 1.5-2.5 Hz. The preprocessed EEG segments, on average, almost equal number of trials in each class per subject were exported to MATLAB, for the single trial feature extraction and classification stages.

D. Feature Extraction

Preprocessed trials from 45 electrode signals over the sensorimotor cortex area were considered; Fig. 3 depicts these electrodes. Each trial was temporally sub-segmented into several overlapping windows. The energies of the bandpassed EEG recordings were computed in each data window and the feature vectors were constructed. The energy features are approximately chi-square distributed, therefore, taking the logarithm makes them almost Gaussian distributed and a linear second order statistics-based classifier such as FLD, see Section III-E, is expected to perform better [27]. Therefore, the classification operations were repeated using the log-energy features of EEGs. The left and right finger movement classification was performed after the feature space dimension reduction using principal component analysis (PCA).

In a further step, in order to accentuate the localized activity and reduce volume conduction effects in multi-channel EEG, the current source density (CSD) transform (available in the BrainVision Analyzer software) was used before computing the features of preprocessed signals. We expect that implementation of the CSD before the feature extracting stage would increase the classifier performance.

E. Classifier Design

The linear discriminant analysis (LDA) classifier based on the Fisher's ratio [28] is utilized here mainly due to its simple computations. For a two-class classification problem, assume that the training patterns is given as $\mathcal{X} = \{\mathbf{x}_1, \mathbf{x}_2, \cdots, \mathbf{x}_l\} = \{\mathcal{X}_1, \mathcal{X}_2\} \subset \mathbb{R}^N$ where the elements of $\mathcal{X}_1 = \{\mathbf{x}_1^1, \mathbf{x}_2^1, \cdots, \mathbf{x}_{l_1}^1\}$ belong to class $\mathcal{L}_1$ and similarly $\mathcal{X}_2 = \{\mathbf{x}_1^2, \mathbf{x}_2^2, \cdots, \mathbf{x}_{l_2}^2\}$ contains patterns from $\mathcal{L}_2$. The FLD computes a vector $\mathbf{w}$ to maximize the between-class distance while minimizing the within-class distance of the feature samples by a linear mapping as $f(\mathbf{x}) = \langle \mathbf{w}.\mathbf{x} \rangle + b$, where $\langle . \rangle$ denotes inner product operator. Vector $\mathbf{w}$ may be computed by maximizing the class separability criterion $J(\mathbf{w})$;

$$\mathbf{w} = \max_{\mathbf{w}} J(\mathbf{w}) = \max_{\mathbf{w}} \frac{\mathbf{w}'\mathbf{S_B}\mathbf{w}}{\mathbf{w}'\mathbf{S_W}\mathbf{w}} \tag{1}$$

where $\mathbf{S_B}$ and $\mathbf{S_W}$ are respectively the between and within class scatter matrices. The bias b of the linear rule is determined using $\langle \mathbf{w}.\mathbf{m}_1 \rangle + b = -(\langle \mathbf{w}.\mathbf{m}_2 \rangle + b)$ and the solution to (1) is $\mathbf{w} = {\mathbf{S_W}}^{-1}(\mathbf{m}_1 - \mathbf{m}_2)$, see [28].

IV. Results

The results of each experiment are reported separately here. For the first experiment, the averaged ssMRPs are first presented. We subsequently report the results of our BCI scheme during the movement initiation and the synchronization states and also during the course of the trials. The effect of the time window size on the BCI performance is then investigated in Section IV-C. We also report the effect of the co-existing transient visual evoked potentials (VEPs) on the ssMRP measurement, ssMRP extension to motor imagery BCI, and separability of ssMRP-based BCI generated without presenting the visual cues.

A. Topographic Analysis of the Averaged EEG Recordings

Of primary interest was the ssMRPs developed during rhythmic tapping. Therefore, bandpass filtered (1.5-2.5 Hz) and current source density (CSD) [29] transformed EEGs recorded during repetitive left and right finger movement trials from the representative subject I were used to visualize the ssMRPs in the time domain. The respective topographic maps, Fig. 4 and Fig. 5, show a rapid development of lateralized rhythmic activity over the contralateral sensorimotor cortex. Topographical maps show snapshots of the spatial distribution of the ssMRPs every 250 ms, that is, at peaks and troughs of 2 Hz rhythm.

B. Classification during Initiation of Rhythmic Tapping

The experiment was designed in such a way that in the first second of each trial, the subjects initiated the rhythmic movement by adopting the correct 2 Hz pace from the visual cues and then continued tapping with the acquired rhythm. Movement initiation may cause EEG activities coming from bilateral or lateralized areas of the brain other than the contralateral sensorimotor cortex which can result in slight degradation in the BCI classification performance. Particularly, these

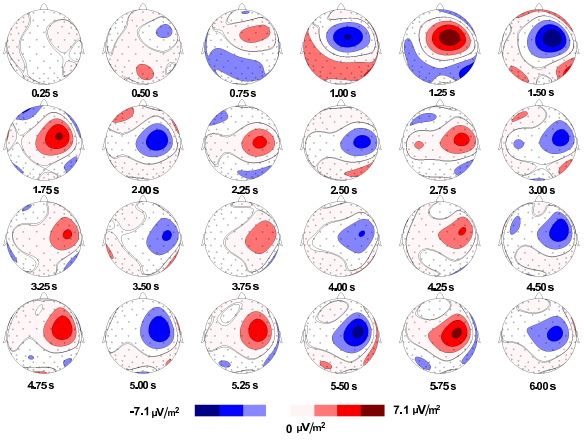

Fig. 4. Averaged pre-processed EEGs during repetitive left finger movement for Subject I. Topographical maps have been depicted in consecutive 0.25 s time windows. The top-left map illustrates the averaged EEGs over 0 and 0.25 seconds time window and the bottom right ones present those of the last 0.25 seconds window, i.e 5.75 to 6 seconds. Notice the rapid development of the lateralized 2 Hz signal on the contralateral right hemisphere.

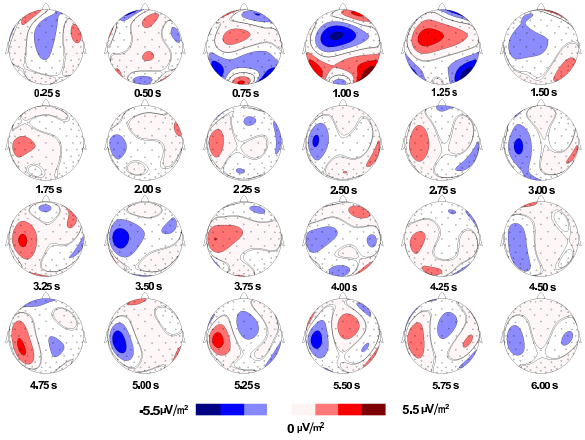

Fig. 5. Averaged pre-processed EEGs during repetitive right finger movement for subject I. Topographical maps have been depicted in consecutive 0.25 s time windows. The top-left map illustrates the averaged EEGs over 0 and 0.25 seconds time window and the bottom right ones present those of the last 0.25 seconds window, i.e 5.75 to 6 seconds. Notice the rapid development of the lateralized 2 Hz signal on the contralateral left hemisphere.

activities may be attributed to potentials generated by frontal structures including pre-supplementary motor area (preSMA) and dorsal premotor cortex (dPMC), engaged during finger selection, movement initiation, and synchronizing to the external cue [24]. In addition, in order to tap in synchrony with the visual stimuli, attending to the visual cues inevitably causes VEPs to be produced by posterior visual areas. Therefore, one would expect that poor classification performance would be achieved during the selection and initiation phases in each trial. The performance should eventually increase after the first second.

In order to investigate how much EEG data should be recorded after the trial onset to have a reliable BCI output, we considered the eight first time intervals, i.e. 0-0.5 s, 0-1 s, 0-1.5 s, 0-2 s, 0-2.5 s, 0-3 s, 0-3.5 s, and 0-4 s. For classification, the 45 electrode signals over the sensorimotor cortex area depicted in Fig. 5 were considered. The feature vector consisted of the (logarithms of the) signal powers at 2 Hz in two conditions: with and without the CSD transform. In order to reduce the dimension of the classifier input space, we used PCA transform and introduced the first three principal components of the feature vectors to the FLD classifier. The classifier was trained on a randomly selected 60% of the resulting reduced feature vectors and tested with the remaining 40%. This cross validation procedure was repeated 400 times. The averaged classification results and their corresponding standard deviations are detailed in Tables I and II.

Note that the first two time intervals, 0-0.5 s and 0-1 s, may be too short to include enough cycles of the 2 Hz rhythm to allow reliable BCI results. However, they can provide an indication of the performance lower bound. The classifier performance eventually increases in later intervals. Tables I and II report that the implementation of the CSD transform increased the CCR for subjects II, IV, and V. However it did not enhance the performance for subjects I and III. Interestingly, for these two subjects the classification results were in an acceptable range in the very early time windows, indicating that following initiation, synchronization stabilized very fast. This might be due to their previous musical training. All subjects had a short training block before the actual recording, nevertheless, they reported afterwards that they had to attend to the pace or the onset of each trial. As expected, Tables I and II report that higher classification results can be achieved if the log-energies of the EEGs are fed to the classifier.

C. Classification through the Trial

After the initiation and the synchronization phases, subjects can keep tapping at almost the exact correct pace. Hence, one could predict that classification based on steady tapping, after the initiation, would be highly reliable. In order to test this finding in the BCI context, we classified the log-energy features of bandpass filtered EEGs in multiple overlapping time windows. Particularly, the discrimination accuracy was compared for three different sliding time window (TW) durations, i.e. $L = 1$ s, $L = 2$ s, and $L = 3$ s and the sliding step was set to 0.125 s. Therefore, for $L = 1$ the TWs were $0-1$ s, $0.125-1.125$ s, $\cdots$, and $5-6$ s, for $L = 2$ they were as $0-2$ s, $0.125-2.25$ s, $\cdots$, and $4-6$ s, and likewise for $L = 3$, the windows $0-3$ s, $0.125-3.125$ s, $\cdots$, and $3-6$ s were considered. Moreover, the ITR [bpm] as the second measure of performance was computed for each time window size according to [13] as

$$\text{ITR [bpm]} = \left[\log_2 N + P\log_2 P + (1-P)\log_2 \frac{1-P}{N-1}\right] \times \frac{60}{L} \tag{2}$$

where $N = 2$ is the number of classes, P is the probability of correct classification, and L is the length of the window in seconds.

The same 45 electrode signals over the sensorimotor cortex area were considered. For each window size, we randomly selected 60% of the computed log-energy feature vectors for FLD training and the remaining 40% of the feature vectors were used for FLD testing. The random selection

TABLE I
AVERAGED CCRS AND THEIR CORRESPONDING STANDARD DEVIATIONS IN [%] DURING MOVEMENT INITIATION; WITHOUT CSD.

Interval vs. Subject	I		II		III		IV		V	
Feature →	E	log(E)	E	log(E)	E	log(E)	E	log(E)	E	log(E)
0 - 0.5 s	78.16 ± 5.3	80.36 ± 4.8	76.37 ± 3.8	76.69 ± 3.8	90.17 ± 2.8	99.40 ± 0.6	56.00 ± 3.1	58.54 ± 3.1	68.94 ± 2.7	59.45 ± 3.1
0 - 1 s	84.79 ± 5.0	88.78 ± 4.0	76.49 ± 3.4	79.16 ± 3.7	97.60 ± 1.5	99.39 ± 0.5	56.65 ± 4.0	80.71 ± 2.9	77.63 ± 2.3	75.96 ± 2.2
0 - 1.5 s	87.46 ± 4.1	88.93 ± 3.6	80.39 ± 3.5	79.60 ± 3.4	95.72 ± 1.8	99.44 ± 0.6	60.58 ± 3.1	86.82 ± 2.1	78.72 ± 2.2	78.59 ± 2.1
0 - 2 s	93.93 ± 2.8	97.75 ± 2.7	70.78 ± 3.9	95.92 ± 2.1	97.43 ± 1.3	99.82 ± 0.3	60.79 ± 3.5	95.75 ± 1.4	82.70 ± 2.1	83.59 ± 1.8
0 - 2.5 s	94.98 ± 2.8	94.48 ± 2.7	69.83 ± 4.2	97.79 ± 1.2	97.63 ± 1.3	100.00 ± 0.0	56.46 ± 3.3	98.49 ± 0.7	83.98 ± 2.0	83.22 ± 2.1
0 - 3 s	93.80 ± 3.1	94.89 ± 2.6	82.36 ± 3.4	97.23 ± 1.5	99.29 ± 0.0	99.93 ± 0.1	50.44 ± 4.2	99.18 ± 0.4	83.24 ± 2.2	80.12 ± 2.2
0 - 3.5 s	91.63 ± 3.4	94.26 ± 1.4	80.44 ± 3.3	85.18 ± 3.2	98.78 ± 0.9	100.00 ± 0.0	75.06 ± 2.6	99.54 ± 0.4	78.68 ± 2.6	80.00 ± 2.2
0 - 4 s	91.61 ± 3.7	99.28 ± 0.9	76.04 ± 3.9	83.38 ± 3.1	98.94 ± 0.9	100.00 ± 0.0	85.86 ± 2.2	99.61 ± 0.3	79.29 ± 2.3	81.11 ± 2.2
Average	89.54	92.34	76.58	86.86	96.94	99.74	62.73	89.83	79.14	77.75

TABLE II
AVERAGED CCR AND THEIR CORRESPONDING STANDARD DEVIATIONS IN [%] DURING MOVEMENT INITIATION; WITH CSD

Interval vs. Subject	I		II		III		IV		V	
Feature →	E	log(E)	E	log(E)	E	log(E)	E	log(E)	E	log(E)
0 - 0.5 s	85.03 ± 3.6	92.61 ± 2.4	73.18 ± 3.7	79.56 ± 3.1	87.14 ± 2.8	96.56 ± 1.5	54.46 ± 3.7	66.84 ± 3.1	65.28 ± 2.4	83.52 ± 2.0
0 - 1 s	87.51 ± 3.0	89.24 ± 2.5	78.05 ± 3.9	81.64 ± 2.8	92.98 ± 2.2	98.81 ± 0.9	91.48 ± 1.2	96.84 ± 1.2	93.55 ± 2.5	99.21 ± 0.2
0 - 1.5 s	78.10 ± 3.7	95.73 ± 1.7	80.14 ± 3.3	94.87 ± 1.7	93.53 ± 2.2	99.98 ± 0.0	95.11 ± 1.7	99.44 ± 0.2	95.18 ± 1.6	99.67 ± 0.0
0 - 2 s	85.00 ± 3.3	98.22 ± 1.1	95.39 ± 1.3	99.33 ± 0.7	96.64 ± 1.2	100.00 ± 0.0	91.62 ± 1.7	99.22 ± 0.2	95.62 ± 1.8	99.56 ± 0.0
0 - 2.5 s	87.74 ± 3.2	98.73 ± 0.9	92.59 ± 2.2	98.19 ± 1.2	97.80 ± 1.3	100.00 ± 0.0	89.68 ± 1.8	99.16 ± 0.7	97.40 ± 1.2	99.30 ± 0.1
0 - 3 s	89.88 ± 0.1	98.18 ± 1.1	94.55 ± 2.1	97.26 ± 1.4	98.51 ± 0.9	99.93 ± 0.1	90.75 ± 1.8	99.60 ± 0.1	97.61 ± 0.9	98.81 ± 0.6
0 - 3.5 s	91.74 ± 2.6	98.11 ± 1.0	93.60 ± 2.0	96.50 ± 2.1	99.07 ± 0.8	100.00 ± 0.0	93.38 ± 2.2	99.26 ± 0.2	98.92 ± 0.2	99.22 ± 0.2
0 - 4 s	95.29 ± 1.8	98.80 ± 1.1	98.99 ± 0.7	99.36 ± 0.3	99.50 ± 0.4	100.00 ± 0.0	93.14 ± 1.7	95.51 ± 0.4	98.74 ± 1.7	99.42 ± 0.2
Average	87.53	96.20	88.31	93.36	95.64	99.41	87.45	94.48	92.78	97.33

TABLE III
AVERAGED CCRS, THEIR CORRESPONDING STANDARD DEVIATIONS IN [%], AND AVERAGED ITRS IN (BPM) AND THE EFFECT OF TIME WINDOW SIZE; WITHOUT CSD

Subject		I		II		III		IV		V		Average
TW		CCR	ITR	CCR	ITR	CCR	ITR	CCR	ITR	CCR	ITR	CCR
1 s	Min	53.93 ± 5.0	0.2	49.93 ± 4.8	0.0	87.94 ± 7.9	28.1	55.28 ± 3.6	0.4	81.72 ± 3.9	18.8	86.09
	Avg	89.21 ± 9.4	30.3	71.70 ± 12.5	8.4	98.50 ± 2.2	53.2	76.01 ± 9.6	12.3	95.03 ± 5.1	42.8	
	Max	98.77 ± 1.4	54.2	99.43 ± 0.7	57.0	99.93 ± 0.0	59.5	95.62 ± 1.3	44.3	99.96 ± 0.0	58.0	
2 s	Min	78.57 ± 4.2	7.5	59.39 ± 4.5	0.7	98.75 ± 0.9	27.0	66.43 ± 3.1	2.3	88.83 ± 2.8	14.8	91.20
	Avg	93.42 ± 5.3	19.5	81.32 ± 10.5	9.1	99.50 ± 0.3	28.6	83.48 ± 9.4	10.6	98.28 ± 2.8	26.2	
	Max	99.52 ± 0.7	28.6	99.62 ± 0.5	28.9	100.00 ± 0.0	30.0	99.05 ± 0.6	27.7	99.69 ± 0.0	29.0	
3 s	Min	88.84 ± 3.2	9.9	68.02 ± 4.6	1.9	98.95 ± 0.7	18.3	76.20 ± 2.8	4.1	99.25 ± 0.1	18.7	93.55
	Avg	96.94 ± 2.9	16.0	82.10 ± 7.6	6.4	99.72 ± 0.3	19.4	89.54 ± 7.5	10.3	99.49 ± 0.1	19.0	
	Max	99.97 ± 0.1	19.9	94.93 ± 1.7	14.2	100.00 ± 0.0	20.0	99.61 ± 0.3	19.2	99.68 ± 0.0	19.3	

and classification procedures were repeated 400 times. We experimentally concluded that the first three principal components of the feature space yields acceptable CCRs for our dataset. Evidently, more advanced pattern classification and dimensionality reduction techniques can be utilized for performance optimization which fall outside the scope of this paper. Tables III and IV summarize the achieved performances. For each time window size and for each subject, the minimum and maximum computed CCRs and ITRs are also reported. As expected, in both Tables III and IV for all five subjects, the averaged CCRs increase when larger time windows are considered. On the other hand, the ITR is inherently influenced by the decision-speed, that is the length of the time window L; the averaged ITRs decrease when L increases. Therefore as for any other BCI mechanism, in ssMRP-based BCI there is a tradeoff between the feature extraction-classification window size and the BCI speed. The utilization of the CSD transform and the logarithm of energy as feature resulted in apparent higher averaged CCRs in Table IV compared to Table III.

D. Transient Visual Evoked Potentials

Brain mechanisms of visual selective attention have been extensively explored by means of VEPs [30]. The VEP is elicited from the extrastriate visual cortex 80-200 ms after a stimulus is presented in an attended location within the subject's visual field [30]. It has been verified [30], [31] that attention to the location where the visual stimulus appears enhances the sensory information and amplifies the consequent

TABLE IV
AVERAGED CCRS, THEIR CORRESPONDING STANDARD DEVIATIONS IN [%], AND AVERAGED ITRS IN (BPM) AND THE EFFECT OF TIME WINDOW SIZE; WITH CSD

Subject		I		II		III		IV		V		Average
TW		CCR	ITR	CCR	ITR	CCR	ITR	CCR	ITR	CCR	ITR	CCR
1 s	Min	56.86 ± 3.5	0.8	65.70 ± 4.2	4.3	95.35 ± 3.8	43.7	74.78 ± 6.9	11.1	76.00 ± 4.6	12.3	
	Avg	70.28 ± 13.0	7.3	93.28 ± 7.7	38.6	98.63 ± 0.9	53.7	89.73 ± 7.5	31.3	96.63 ± 4.4	47.2	89.71
	Max	90.46 ± 2.2	32.7	99.60 ± 0.5	57.7	99.74 ± 0.2	58.4	99.52 ± 0.1	57.4	100.00 ± 0.0	60.0	
2 s	Min	50.99 ± 4.4	0.0	79.95 ± 3.9	8.3	97.99 ± 1.5	25.7	82.28 ± 5.4	9.7	94.85 ± 3.1	21.2	
	Avg	82.61 ± 3.2	10.0	97.46 ± 3.8	24.8	99.23 ± 0.6	28.0	94.98 ± 5.1	21.3	98.93 ± 1.0	27.4	94.64
	Max	93.50 ± 2.1	19.6	99.63 ± 0.5	28.9	100.00 ± 0.0	30.0	99.49 ± 0.2	28.5	100.00 ± 0.0	30.0	
3 s	Min	71.40 ± 4.0	2.7	86.39 ± 3.3	8.5	98.81 ± 0.8	18.1	94.63 ± 1.4	13.9	98.14 ± 0.4	17.3	
	Avg	85.56 ± 6.8	8.0	97.74 ± 3.0	16.8	99.66 ± 0.4	19.3	98.03 ± 1.5	17.2	99.00 ± 0.2	18.3	95.99
	Max	94.46 ± 2.1	13.8	99.64 ± 0.5	19.3	100.0 ± 0.0	20.0	99.63 ± 0.1	19.3	99.52 ± 0.1	19.1	

VEP.

In the context of our BCI protocol, we instructed the subject to fixate on the central cross, and not on the lateralized visual pacing cues. This approach attenuates the VEPs considerably. In Section IV-B, we mentioned that the subjects of the first experiment reported that they had to attend the visual cues at the beginning of each trial which could lead to VEPs that lowered the classification performance in the first second of each trial, Table I and Table II.

In order to verify the correspondence between the attenuation of the VEPs and gradually improving CCRs, we monitored VEPs during the first two seconds of each trial (Fig. 4). In that two seconds period, four visual stimuli were presented to the subject and each was followed by a VEP after approximately 170 ms. Fig. **??** depicts the averaged VEPs across the period for electrode PO7, PO8, C3, and C4. The corresponding full scale topographical distributions at times 0.42 s, 0.92 s, 1.42 s, and 1.92 s are plotted in Fig. **??** to Fig. **??**. Importantly, note the large amplitude of the first VEP and the attenuation of the following VEPs at PO8. This rapid attenuation would greatly reduce VEP contamination of ssMRPs after the first second. Moreover, either in the absence of or during a motor act the VEPs are largely confined to the visual cortex (Fig. **??** to Fig. **??**). Therefore for BCI, VEP contamination of ssMRPs recorded from the motor cortex should be limited to only the beginning of each trial.

E. Imagination of rhythmic tapping for BCI

Cortical signals produced during overt or covert movements present similar spatio-temporal patterns as the motor cortex behaves in similar ways during both. In [32], it was shown that rhythmic imagination of left and right finger movements with frequencies greater than 1 Hz modulates cortical potentials and leads to ssMRPs. However in rhythmic motor imagination, it is not possible to objectively verify whether the subject could successfully maintain the correct pace. Osman *et al.* in [32] showed that high frequency rhythmic motor imagination can be carried out after extensive subject training in real rhythmic motor actions.

We tested whether classification of ssMRPs recorded during rhythmic finger movement imagination is feasible for BCI applications. Hence, in the second experiment the subject was instructed to repetitively imagine left or right finger movements after the early fixation period and adopting the correct pace after fixation at the beginning of each trial, see Fig. 4. The same classification procedure using two time windows of lengths 1 s and 2 s was carried out. The averaged CCRs, their corresponding standard deviations, and the ITRs are shown in Table V. The relatively high classification rates of about 90.2% and 93.4%, respectively when the time window was 1 s or 2 s, demonstrate the applicability of the ssMRPs for motor imagery- based BCI. Note that as in Section IV-C, using a wider time window enhances the classification performance, but reduces the ITR.

TABLE V
AVERAGED CCRS, THEIR CORRESPONDING STANDARD DEVIATIONS IN [%], AND AVERAGED ITRS IN (BPM) FOR THE SECOND DATASET

Period		Motor Imagery		Without Cue	
TW		CCR	ITR	CCR	ITR
1 s	Min	83.47 ± 7.2	21.1	63.16 ± 6.1	3.0
	Avg	90.21 ± 3.2	32.2	81.36 ± 7.1	9.1
	Max	91.56 ± 0.9	34.9	95.92 ± 2.6	45.2
2 s	Min	92.78 ± 1.1	18.7	72.38 ± 5.0	4.5
	Avg	93.49 ± 0.4	19.5	84.79 ± 8.7	23.1
	Max	95.12 ± 0.4	21.5	98.44 ± 2.9	26.5

F. Extension to BCI without Visual Cue

All established BCI approaches require external visual or audio cues to certain levels. For instance the ssVEP- or P300-based BCI would not be possible without the visual stimuli. However, the ssMRPs can be generated without the visual cues after the subjects adopt the correct pace. As shown in Fig. 4, in the fourth part of each trial the subject started to rhythmically tap but without the rhythmic visual cue. Then, the subject was asked to continue tapping in the fifth period for another 2 seconds when the cues appeared.

The participant's success at tapping with the correct rhythm is reflected in Fig.7 which displays the time between successive taps (inter-tap intervals). The fourth and the fifth periods included respectively 6 and 4 taps and hence 5 and 3 intervals. Fig. 7 reports that the subject maintained a pace of approximately 2.2 Hz. Moreover, these results match our

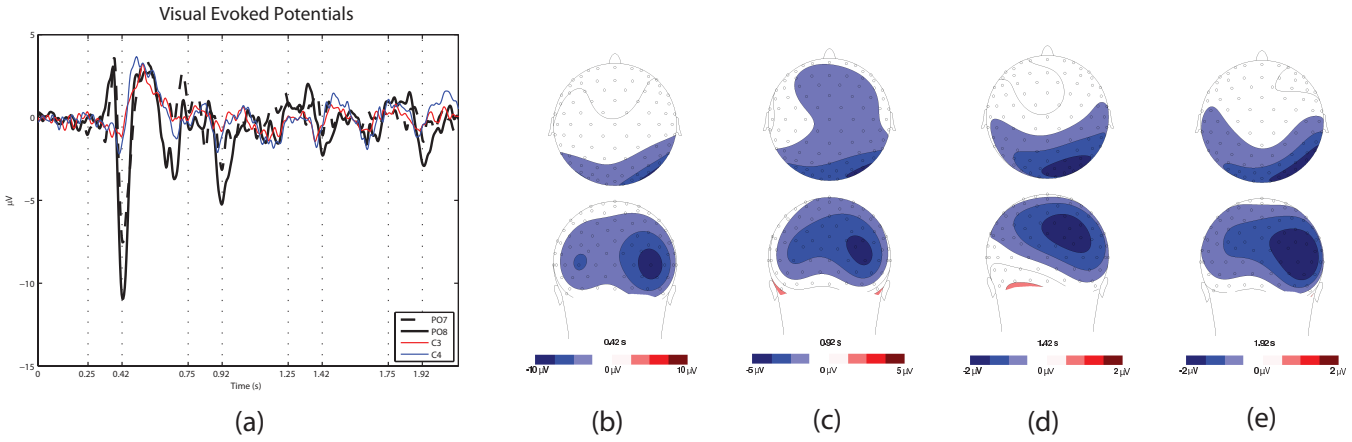

Fig. 6. The spatio-temporal patterns of VEPs recorded during the first four seconds of each trails; (a) The averaged VEPs from four representative electrodes in Time; (b) the topographical distribution of first VEP at 0.42 ms approximately 0.17 ms after the first visual cue; (c)-(e) the topographical distributions of the subsequent VEPs. Note the change in amplitude scaling of the topographic maps in (b)-(e).

earlier findings that once a fast rhythmic action is started it can be carried out almost automatically [24].

As before, two different time windows of 1 s and 2 s were considered and the pattern classification procedure was implemented; the results are reported in Table V. Note that, the averaged CCRs during the "Tapping Without Cue" are relatively lower than that of "Motor Imagery". This can be explained as transition from motor imagination to real movement could activate brain areas other than sensorimotor cortex and consequently a transient drop in the CCRs. Another potential cause could be the replacement of the central fixation cross with an "X" for about 100 milliseconds which elicits a VEP. As we utilize no spatial filtering to attenuate the effect of this VEP, deterioration of the CCRs are inevitable.

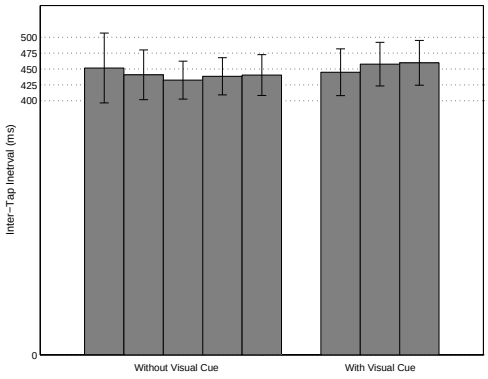

Fig. 7. Distribution of inter-tap intervals (time between successive taps) without and with the visual cues. Error bars show the standard deviations.

V. Conclusions

The present study used the ssMRPs to provide a measure of sensorimotor cortex activation during rhythmic tapping and suggested a potential application for a real-time high accuracy BCI. In this approach the subjects were asked to cyclically move their left or right index fingers at a pre-determined frequency. Therefore, the lateralized and band limited ssMRP was detected from the sensorimotor cortex. The main advantage of the ssMRP-based BCI over other approaches is its simple recording setup and straightforward computations. Comparing to BCI machines based on RPs, using the ssMRP for BCI would not be difficult for the subjects since in each trial they are actively involved in the experiment, rather than waiting for several seconds before the exertion of a single discrete movement.

Here, the ssMRP-based BCI has been tested for six healthy subjects. However, its physiological background and simplicity of the recording setup support the repeatability of the experiments. In the first experiment, the maximum performance was attained for data windows lying in the middle of each trial, at approximately 3-4 seconds after the movement onset in each trial for all participants. For most subjects reliable classification rates could be achieved with shorter data lengthes and the average CCR for a data window of only 2 s with (or without) the CSD transform was 94.6% (or 91.2%).

The use of CSD transform and the log-energy features increased the performance. However, in order to test whether that increase is statistically significant more subjects are needed. On the other hand, real-time implementation of such non-linear transformation is not trivial. A simpler approach would be to incorporate the Laplacian derivative of EEGs at each electrode site which is the second derivative of the spline function at that location. Similar to the CSD transform, it is related to the rate of change over space and amplifies the contribution of nearby electrical sources and diminishes that of distant ones.

We argue that the ssMRP-based BCI is simpler than the ssVEP-based BCI systems in terms of subject training time and signal analysis. In the proposed method, advanced spectral estimation algorithms are not necessary since instead of frequency separation of ssVEP, only one frequency is dealt with. In other words, instead of exploiting the spectral disparity in the signal processing unit of the BCI machine, the topographical distribution of scalp EEG signals in the frequency band of interest is used to identify the effector. The ssMRP approach for BCI can be extended beyond the present example in a number of ways. To begin with, it should be possible to realize all the ssVEP-based applications by the ssMRPs where

a continuous BCI signal rather than a chain of discrete outputs is needed; a prime example is robot or wheelchair navigation. Second, the large number of electrodes utilized in this research should not generally be regarded as a hindrance towards end-product BCI and acceptable performance can be expected from fewer electrodes situated over the two motor cortices (Fig. 5).

There is subtle difference here between our interpretation of the ssMRPs and that of Gerloff *et al.* in [21] where each tap was treated individually for exploring EEG correlates of sensorimotor activity around the tap onset. However, in our work we treat taps in a short train, i.e. in windows of one, two, or three seconds, and search for their EEG signatures. On the other hand, a challenging research question would be the classification of ssMRPs but on the classic tap-by-tap basis which effectively follows [8] and [12]. In [21] it was shown that the averaged tap-by-tap segmented ssMRPs show distinct pre-movement motor and post-movement sensory components. For the pre-movement component, one would expect to identify a radial dipole source in the primary motor cortex contralateral to the side of the movement followed by a tangential post-movement source located in the primary sensory cortex slightly inferior to the former source. These two sources would reflect the repetitive efferent and re-afferent motor outputs and sensory inputs. Therefore, capturing such a pre-movement EEG negative signatures of centro-parietal activity followed by a complex of "frontal negative"-"parietal positive" EEG distribution can significantly enhance the performance of the ssMRP-based BCI if it can be realized for the single trial data.

Note that there are also certain differences between our recording setup and those of previous studies such as [8] and [12] where the participants could alternate between right and left fingers in consecutive short intervals. That is, the subject could decide whether to move the left or right index on each tap. In [8] and [12], the participants were not provided with rhythmic visual cues and therefore a series of discrete movements were carried out rather than rhythmic continuous movements. Therefore, as discussed in Section II, the lower classification performances they obtained might be due to the repetitive activation of the frontal cortex during the initiation of each discrete movement. In [8] the actual number of taps per hand and the inter-hand transition matrix had to be computed objectively and shown on the screen; the taps on the keyboard were extracted as markers into the stream of EEG measurements. Therefore, if the tap rate or the number of alterations deviated from pre-instructed rate, the subject was informed so those could be compensated accordingly. In such a scenario, one could not expect steady state MRPs to be generated. Finally, In specific applications, such as typing on the keyboard, the BCI system should ideally be able to distinguish between left and right finger movements in each individual discrete tap. However, there are other applications such as navigating a wheelchair, in which a smooth and continuous BCI output is demanded. We believe that with further refinements our protocol will lead to a reliable and robust BCI.

Acknowledgement

The authors would like to acknowledge Dr. Benjamin Blankertz at Berlin BCI for his comments on EEG recording protocol used in [8] and [12].

References

[1] M. Jahanshahi and M. Hallet, eds., *The Bereitschaftspotential Movement-Related Cortical Potentials*. Kluwer Academic, 2003.

[2] R. Q. Cui, D. Huter, W. Lang, and L. Deecke, "Neuroimage of voluntary movement: Topography of the Bereitschaftspotential, a 64-channel DC current source density study," *NeuroImage*, vol. 9, pp. 124–134, 1999.

[3] M. G. H. Coles, H. G. O. M. Smid, M. K. Scheffers, and L. J. Otten, *Mental chronometry and the study of human information processing*, ch. Electrophysiology of mind: event-related brain potentials and cognition In M. D. Rugg and M. G. H. Coles (Ed.), pp. 86–131. Oxford: Oxford University Press, 1995.

[4] P. Praamstra, D. F. Stegeman, A. R. Cools, and M. W. I. M. Horstink, "Reliance on external cues for movement initiation in Parkinson's disease; evidence from movement-related potentials," *Brain*, vol. 121, pp. 167–177, 1998.

[5] M. Kustas and E. Donchin, "Preparation to respond as manifested by movement-related brain potentials," *Brain Research*, vol. 202, pp. 95–115, 1980.

[6] M. G. H. Coles and G. Gratton, *Cognitive psycophysiology and the study of states and processes*, ch. Energetic and Human Information Processing In G. R. J. Hockey and A. W. K. Gaillard and M. G. H. Coles (Eds.), pp. 409–424. Dordrecht, The Netherlands: Martinus Nijhof, 1986.

[7] T. Hinterberger, S. Schmidt, N. Neumann, J. Mellinger, B. Blankertz, G. Curio, and N. Birbaumer, "Brain-computer communication with slow cortical potentials," *IEEE Trans. Biomed. Eng.*, vol. 51, no. 6, pp. 1011–1018, 2004.

[8] B. Blankertz, G. Dornhege, M. Krauledat, K.-R. Müller, V. Kunzmann, F. Losch, and G. Curio, "The Berlin Brain Computer Interface: EEG-Based communication without subject training," *IEEE Trans. Neur. Sys. Rehab. Eng.*, vol. 14, pp. 147–152, 2006.

[9] B. Blankertz, G. Dornhege, C. Schäfer, R. Krepki, K.-R. Müller, V. Kunzmann, F. Losch, and G. Curio, "Boosting bit rates and error detection for the classification of fast-paced motor commands based on single-trial EEG analysis," *IEEE Trans. Neur. Sys. Rehab. Eng.*, vol. 11, no. 2, pp. 127–131, 2003.

[10] R. Krepki, B. Blankertz, G. Curio, and K.-R. Müller, "The Berlin brain-computer interface (BBCI) - towards a new communication channel for online control in gaming applications," *Journal of Multimedia Tools and Applications*, vol. 33, pp. 73–90, 2007.

[11] R. Krepki, G. Curio, B. Blankertz, and K.-R. Müller, "Berlin brain-computer interface - the HCI communication channel for discovery," *Int. J. Hum. Comp. Studies, Special Issue on Ambient Intelligence*, vol. 65, pp. 460–477, 2007.

[12] B. Blankertz, G. Dornhege, S. Lemm, M. Krauledat, G. Curio, and K.-R. Müller, " The Berlin Brain-Computer Interface: Machine learning based detection of user specific brain states," *J Universal Computer Sci*, vol. 12, pp. 581–607, 2006.

[13] J. R. Pierce, *An Introduction to Information Theory*. New York: Dover, pp. 145165, 1980.

[14] G. Dornhege, B. Blankertz, G. Curio, and K.-R. Müller, "Boosting bit rates in non-invasive EEG single-trial classifications by feature combination and multi-class paradigms," *IEEE Trans. Biomed. Eng.*, vol. 51, no. 6, pp. 993–1002, 2004.

[15] D. Regan, *Human Brain Electrophysiology: Evoked Potentials and Evoked Magentic Fields in Science and Medicine*. Amsterdam, The Netherlands: Elsevier, 1989.

[16] G. R. McMillan, G. L. Calhoun, M. S. Middendorf, J. H. Schnurer, D. F. Ingle, and V. T. Nasman, "Direct brain interface utilizing selfregulation of steady-state visual evoked response (SSVER)," in *Proc. RESNA95*, pp. 693–695, USA, 1995.

[17] G. R. Müller-Putz, R. Scherer, C. Brauneis, and G. Pfurtscheller, "Steady-state visual evoked potential (SSVEP)-based communication: impact of harmonic frequency components," *J. Neural Eng.*, vol. 2, pp. 123–130, 2005.

[18] P. Martinez, H. Bakardjian, and A. Cichocki, "Fully online multi-command brain-computer interface with visual neurofeedback using SSVEP paradigm," *Computational Intelligence and Neuroscience*, 2007. doi:10.1155/2007/94561.

[19] S. P. Kelly, E. C. Lalor, R. B. Reilly, and J. J. Fox, "Visual spatial attention tracking using high-density SSVEP data for independent Brain-Computer communications," *IEEE Trans. Neural Sys. Rehab. Eng.*, vol. 13, no. 2, pp. 172–178, 2005.

[20] B. H. Repp, "Rate limits of sensorimotor synchronization," *Advances in Cognitive Psychology*, vol. 2, pp. 163–181, 2006.

[21] C. Gerloff, C. Toro, N. Uenishi, L. G. Cohen, L. Leocani, and M. Hallett, "Steady-state movement-related cortical potentials: a new approach to assessing cortical activity associated with fast repetitive finger movements," *Electroencephal. Clin. Neurophysiol.*, vol. 102, pp. 106–113, 1997.

[22] P. A. Lewis and R. C. Miall, "Distinct systems for automatic and cognitively controlled time measurement: evidence from neuroimaging," *Current Opinion in Neuribiology*, vol. 13, pp. 250–255, 2003.

[23] R. C. Miall and R. Ivry, "Moving to a different beat," *Nat. Neuroscience*, vol. 7, no. 10, pp. 7–8, 2004.

[24] P. A. Lewis, A. M. Wing, P. A. Pope, P. Prammstra, and R. C. Miall, "Brain activity correlates differentially with increasing temporal complexity of rhythms during selection, synchronisation, and continuation phases of paced finger tapping," *Neuropsychologia*, vol. 42, pp. 1301–1312, 2004.

[25] S. Schaal, D. Sternad, R. Osu, and M. Kawato, "Rhythmic arm movement is not discrete," *Nature Neuroscience*, vol. 7, no. 10, pp. 1137–1144, 2004.

[26] R. Oostenveld and P. Praamstra, "The five percent electrode system for highresolution EEG and ERP measurements," *Clin. Neurophysiol.*, vol. 112, pp. 713–719, 2001.

[27] B. Blankertz, M. Kawanabe, R. Tomioka, F. Hohlefeld, V. Nikulin, and K.-R. Müller, "Invariant common spatial patterns: Alleviating nonstationarities in brain-computer interfacing," in *Proc. NIPS, 20, MIT Press*, USA, 2008.

[28] K. Fukanaga, *Introduction to Statistical Pattern Recognition*. Academic, 2nd ed., 1990.

[29] F. Perrin, J. Pernier, O. Bertrand, and J. Echallier, "Spherical splines for scalp potential and current density mapping," *Electroencephal. Clin. Neurophysio.*, vol. 72, pp. 184–187, 1989.

[30] M. I. Posner and S. Dehanaene, "Attentional networks," *Trends in Neuroscince*, vol. 17, no. 2, pp. 1643–1650, 1994.

[31] S. T. Morgan, J. C. Hansen, and S. Hillyard, "Selective attention to stimulus location modulates the steady-state visual evoked potential," *PNAS USA*, vol. 93, pp. 4770–4774, 1996.

[32] A. Osman and R. Albert and K. R. Ridderinkhof and G. Band and M. van der Molen, "The beat goes on: rhythmic modulation of cortical potentials by imagined tapping.," *JEP-HPP*, vol. 32, no. 4, pp. 986–1005, 2006.